Dynamics of Gas-phase Hydrogen Atom Reaction with Chemisorbed Hydrogen Atoms on a Silicon Surface

Sun-Hee Lim, Jongbaik Ree, and Yoo Hang Kim†,*

Department of Chemistry Education, Chonnam National University, Kwangju 500-757, Korea
†Department of Chemistry and Center for Chemical Dynamics, Inha University, Inchon 402-751, Korea
Received June 11, 1999

The collision-induced reaction of gas-phase atomic hydrogen with hydrogen atoms chemisorbed on a silicon (001)-(2×1) surface is studied by use of the classical trajectory approach. The model is based on reaction zone atoms interacting with a finite number of primary system silicon atoms, which then are coupled to the heat bath, *i.e.*, the bulk solid phase. The potential energy of the $H_{ads}\cdots H_{gas}$ interaction is the primary driver of the reaction, and in all reactive collisions, there is an efficient flow of energy from this interaction to the H_{ads}-Si bond. All reactive events occur on a subpicosecond scale, following the Eley-Rideal mechanism. These events occur in a localized region around the adatom site on the surface. The reaction probability shows the maximum near 700 K as the gas temperature increases, but it is nearly independent of the surface temperature up to 700 K. Over the surface temperature range of 0-700 K and gas temperature range of 300 to 2500 K, the reaction probability lies at about 0.1. The reaction energy available for the product states is small, and most of this energy is carried away by the desorbing H_2 in its translational and vibrational motions. The Langevin equation is used to consider energy exchange between the reaction zone and the bulk solid phase.

Introduction

In the past three decades, researchers have shown that it is possible to direct gas-phase reactants toward adsorbed species on well characterized surfaces and determine the outcome of interaction events by use of spectroscopic techniques.[1-3] Such studies have produced valuable information about the chemical and physical properties of adsorbed layers, and this information is essential for the development of fundamental concepts on gas-surface reactions. In recent years a surge of research activity has occurred both experimentally and theoretically in the field of gas-surface interactions, and surface science embracing this field is fast reaching maturity.[1-4] Among the solid surfaces studied in recent years is silicon, which is at the heart of our information age.[5-26] The chemisorption of hydrogen atoms on a silicon surface occurs during important surface processing techniques. Understanding the physical properties and chemical reactivities of these adatoms is of major importance in the development of silicon-related materials and silicon-surface assisted reactions. One such problem is the removal of the adatoms by the incident gas atoms, such as hydrogens and halogens, in which case the reaction probability and product energy distributions are among the important problems to be studied. An important type of such reactions is the interaction of gas-phase atomic hydrogen with chemisorbed hydrogen atoms, $H(g) + H(ad)/Si \rightarrow H_2(g) + Si$, which has received a considerable attention in recent years.[11,12,17-26]

In such gas-adatom interactions, the reaction is initiated by the incidence of gas phase atoms which are not in equilibrium with the surface. Therefore, the resulting reactive events in this collision-induced process follow the Eley-Rideal (ER) mechanism. The ER mechanism has been considered to be much less common than the Langmuir-Hinshelwood (LH) type.[2] In the collision-induced process, the dynamics of energy flow between the gas-adatom interaction and the adatom-surface vibration, adatom-surface bond dissociation, and gas-adatom bond formation are problems of fundamental importance in understanding the details of such reactions.

The purpose of this paper is to study the reaction of gas-phase atomic hydrogen with chemisorbed hydrogen atoms on silicon(001)-(2×1) surface with particular reference to the problem of product energy distribution. To study the reaction, we shall follow the time evolution of the pertinent coordinates and conjugate momenta of each reactive event on a potential energy surface, which is constructed with many-body interactions operating between all atoms of the reaction system. The time evolution will be determined by the solution of the equations of motion formulated by uniting gas-surface procedure and generalized Langevin theory for the solid phase.[27-29] The dynamics study will provide an answer to the following questions: How long does it take for the adatom-surface bond to break and H_2 product molecule to form? How is the available reaction energy disposed of among the various degrees of freedom of the product molecule? How are the reaction probabilities dependent upon the gas and the surface temperatures? We will pay our attention mainly on the reaction taking place at the gas temperature of 1800 K and the surface temperature of 300 K, which are typical experimental conditions. However, a brief discussion of the temperature dependence of reaction at other gas and surface temperatures will also be presented.

Model and Numerical Procedures

The interaction model and numerical procedures have already been reported in detail in Ref. 30. We summarize the

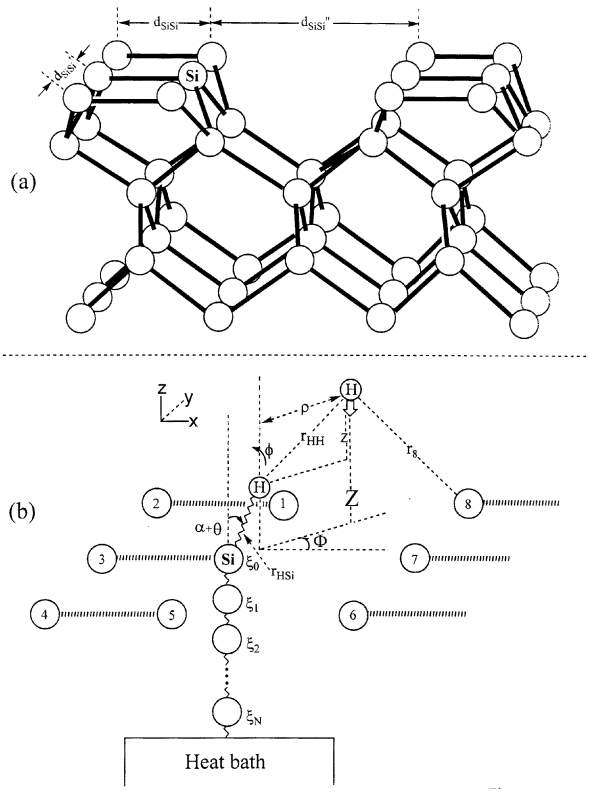

Figure 1. (a) Symmetric Si-Si dimer surface. $d_{Si\text{-}Si}$ 2.52 Å. $d_{Si\text{-}Si'}$ = 3.87 Å, $d_{Si\text{-}Si''}$ = 5.15 Å. (b) Interaction model showing the H_{ads} atom adsorbed on the 0th Si atom, which is coupled to the N-atom chain. The coordinates of the (N−1) chain atoms including the 0th atom are denoted by $\xi_0, \xi_1, \ldots, \xi_N$. The 0th atom is indentified by Si in both Figs. (a) and (b). The Nth atom of the chain is coupled to the heat bath. The position of H_{ads} is identified by (r_{HSi}, θ, ϕ) and the position of H_{gas} by (ρ, Z, Φ). α is the tilt angle. The H_{gas} to H_{ads} distance is denoted by r_{HH}, and the H_{gas} to the ith surface-layer Si atom distance by r_i.

essential aspects of the interaction on the silicon (001)-(2×1) surface reconstructed by forming dimers along the [110] direction (Figure 1a). We have displayed the collision model in Figure 1b, which is the same as that in Ref. 30 except the fact that the adsorbed chlorine atom is replaced by the hydrogen atom. The reaction zone is composed of the incident hydrogen atom(hereafter called as H_{gas}), the adsorbed hydrogen atom(hereafter called as H_{ads}), and the 0th Si atom. The 0th atom is coupled to the N-atom chain, which then links the reaction zone to the heat bath, providing a simple quasiphysical picture of energy flow between the reaction zone and the chain atoms and in turn between the chain and the heat bath. We include all these strongly interacting reaction zone atoms, surface atoms and N-chain atoms in the primary system. We then designate the remaining infinite number of solid atoms as secondary atoms. If we restrict the collision system only to the gaseous H atom, the adsorbed H atom and the rigid solid with infinite mass, we can perform a rigorous quantum mechanical scattering calculation. Our collision model, however, comprises many more atoms. In addition to the H atoms, there are nine surface layer Si atoms, N chain atoms (N is typically eight to ten) and the remaining solid bulk acting as the heat bath. For this kind of large, realistic collision system quantum mechanical calculation is out of question, and we employ classical trajectory studies.

It is also interesting to note that our model includes N-chain atoms, which link the reaction zone to the heat bath solid atoms, in the primary system, whereas the model described by Kratzer doesn't include these atoms even though he also employed the classical calculation.[17] Since this model includes heat bath, the primary system is coupled to the heat bath, which exerts a systematic dissipative force on the primary system. In addition to this dissipative force, the heat bath also exerts a random or stochastic force on the primary system. When the solid is at $T_s > 0$ K, it can either gain energy from or lose energy to the reaction region, so the random force may either remove energy from or provide energy to the primary system. By including heat bath in our model, therefore, we can study the reaction taking place at an arbitrary solid temperature.

The gas atom approaches the surface with the initial collision energy E and impact parameter b. It experiences strong interactions with the adatom and many surface atoms. During the collision, the H_{gas} to H_{ads} interaction is strengthened to a sufficient level to form a $H_{gas}\cdots H_{ads}$ bond, while the H_{ads}-Si surface bond is weakened and eventually dissociates. Although the energy of these interactions is of primary importance in determining the extent of reaction, the potential energies resulting from the nearby Si atoms which surround the 0th Si atom can affect the outcome of the collision event. In the model, thus, we consider the 0th Si atom of the chain to be surrounded by eight nearby Si atoms of the symmetric dimer strands, and we include the resulting interactions between them and the gas atom in constructing the potential energy surface (PES).

We express the interaction energy as an explicit function of the positions of the incident gas atom H_{gas}, adatom H_{ads}, and primary zone solid atoms. We define Z to be the distance of the gas atom from the surface in the normal direction, r_{HSi} to be the distance of the adatom H_{ads} from the surface site describing the stretching vibration of the inclined H_{ads}-Si bond, r_i to be the distance between the gas atom and the ith silicon atom on the surface layer (i = 0, 1, ..., 8), and ξ_j to be the vibrational displacement of the jth atom of the N-atom chain (j = 0, 1, 2, ..., N) from its equilibrium position. A total of six degrees of freedom is necessary to describe the motions of H_{gas} and H_{ads} atoms above the surface. The H_{ads} coordinates are $x_a = r_{HSi}\sin(\alpha + \theta)\cos\phi$, $y_a = r_{HSi}\sin(\alpha + \theta)\sin\phi$, and $z_a = r_{HSi}\cos(\alpha + \theta)$, *i.e.*, $H_{ads}(x_a, y_a, z_a) - H_{ads}(r_{HSi}, \theta, \phi)$. Prior to dissociation, the restricted motion of the adatom around its equilibrium position from the 0th Si atom will be described by the tilt angle α and the hindered rotational angles θ and ϕ. The literature value of the tilt angle is 20.6°.[31] For the position of H_{gas} with respect to the reference axes along the adatom, we note that the $H_{gas}\cdots H_{ads}$ interatomic distance r_{HH} is $(\rho^2 + z^2)^{1/2}$, where the initial ($t \to -\infty$) value of ρ is the impact parameter b. The projection of r_{HH} on the surface plane is oriented by the angle Φ from the X

axis. Thus, the coordinate (x_g, y_g, z_g) transforms into the cylindrical coordinate system (ρ, Z, Φ). The distance z displayed in Figure 1 is then $z = Z - r_{HSi}\cos(\alpha+\theta)$. Thus the occurrence of reactive events can be determined by studying the time evolution of the H_{ads}-Si bond distance r_{HSi} and the $H_{gas}\cdots H_{ads}$ distance $r_{HH}=(\rho^2+z^2)^{1/2}$ for the ensemble of gas atoms approaching the surface from all possible directions.

Any rigorous form of the interaction potential should include all those interactions mentioned above. For the overall interaction energy, we first take a modified form of the London-Eyring-Polanyi-Sato (LEPS) potential energy surface (PES)[30] for the interactions of H_{gas} to H_{ads}, H_{gas} to Si, H_{ads} to Si, and H_{gas} to the eight surface layer atoms, all of which are considered to be exponential. Then, we combine this modified form with the θ- and ϕ-hindered rotational motions and the harmonic motions of the (N+1)-chain atoms:

$$U(r_{HH}, r_{HSi}, Z, \{r\}, \{\xi\}) = \{Q_{HH} + Q_{HSi} + Q_{HS} - [A^2_{HH} + A^2_{HSi} + A^2_{HS} - A_{HH}A_{HSi} - (A_{HH} + A_{HSi})A_{HS}]^{1/2}\} + 1/2k_\theta(\theta-\theta_e)^2 + 1/2k_\phi(\phi-\phi_e)^2 + \Sigma(1/2M_s\omega_{cj}^2\xi_j^2) + \Sigma(\text{terms of type } 1/2M_s\omega_{cj}^2\xi_{j-1}\xi_j,\ 1/2M_s\omega_{c,j+1}^2\xi_j\xi_{j+1}, \text{ etc.}), \quad (1)$$

where k_θ, k_ϕ are the force constants, θ_e and ϕ_e are the equilibrium angles, M_s is the mass of the silicon atom, ω_{cj} is the Einstein frequency, and ω_{sj} is the coupling frequency characterizing the chain. The explicit forms of the Q's and A's are

$$Q_k = 1/4[D_k(1+\Delta_k)][(3+\Delta_k)e^{(r_{ke}-r_k)/a_k} - (2+6\Delta_k)e^{(r_{ke}-r_k)/2a_k}], \quad (2a)$$

$$A_k = 1/4[D_k(1+\Delta_k)][(1+3\Delta_k)e^{(r_{ke}-r_k)/a_k} - (6+2\Delta_k)e^{(r_{ke}-r_k)/2a_k}], \quad (2b)$$

for k = HH or HSi, $\{\xi\} = (\xi_0, \xi_1, \ldots, \xi_N)$ and $\{r\} = (r_0, r_1, \ldots, r_8)$. The H_{gas}-surface (HS) energy is composed of the nine terms including the contribution of the H_{gas} to 0th Si atom interaction:

$$Q_{HS} = [D_{HS}(1+\Delta_{HS})]\{\sum_{i=0}^{8}[(3+\Delta_{HS})e^{(r_{ie}-r_i)/a_{HS}} - (2+6\Delta_{HS})e^{(r_{ie}-r_i)/2a_{HS}}]\} \quad (3a)$$

$$A_{HS} = [D_{HS}(1+\Delta_{HS})]\{\sum_{i=0}^{8}[(1+3\Delta_{HS})e^{(r_{ie}-r_i)/a_{HS}} - (6+2\Delta_{HS})e^{(r_{ie}-r_i)/2a_{HS}}]\} \quad (3b)$$

where,

$r_0^2 = Z^2 + (\rho\sin\Phi + r_{HSi}\sin\phi)^2 + [r_{HSi}\sin(\alpha+\theta) + \rho\cos\Phi]^2$,

$r_1^2 = Z^2 + (d'_{SiSi} - r_{HSi}\sin\phi - \rho\sin\Phi)^2 + [r_{HSi}\sin(\alpha+\theta) + \rho\cos\Phi]^2$,

$r_2^2 = Z^2 + (d'_{SiSi} - r_{HSi}\sin\phi - \rho\sin\Phi)^2 + [d_{SiSi} + r_{HSi}\sin(\alpha+\theta) + \rho\cos\Phi]^2$,

$r_3^2 = Z^2 + (\rho\sin\Phi + r_{HSi}\sin\phi)^2 + [d_{SiSi} + r_{HSi}\sin(\alpha+\theta) + \rho\cos\Phi]^2$,

$r_4^2 = Z^2 + (d'_{SiSi} + r_{HSi}\sin\phi + \rho\sin\Phi)^2 + [d_{SiSi} + r_{HSi}\sin(\alpha+\theta) + \rho\cos\Phi]^2$,

$r_5^2 = Z^2 + (d'_{SiSi} + r_{HSi}\sin\phi + \rho\sin\Phi)^2 + [r_{HSi}\sin(\alpha+\theta) + \rho\cos\Phi]^2$,

$r_6^2 = Z^2 + (d'_{SiSi} + r_{HSi}\sin\phi + \rho\sin\Phi)^2 + [d''_{SiSi} + r_{HSi}\sin(\alpha+\theta) + \rho\cos\Phi]^2$,

$r_7^2 = Z^2 + (\rho\sin\Phi + r_{HSi}\sin\phi)^2 + [d''_{SiSi} + r_{HSi}\sin(\alpha+\theta) + \rho\cos\Phi]^2$,

$r_8^2 = Z^2 + (d'_{SiSi} - r_{HSi}\sin\phi - \sin\Phi)^2 + [d''_{SiSi} + r_{HSi}\sin(\alpha+\theta) + \rho\cos\Phi]^2$.

Here, D_k and a_k are usual Morse potential parameters. r_{ke} is the equilibrium value of the distance r_k, and Δ_k is the adjustable Sato parameter that allows a variety of experimental situations to be modeled. Since $r_i = r_i(r_{HSi}, \theta, \phi, \rho, Z, \Phi)$ and $r_{HH} = r_{HH}(r_{HSi}, \theta, \rho, Z)$, the potential energy surface has the functional dependence of $U(r_{HSi}, \theta, \phi, \rho, Z, \Phi, \{\xi\})$.

The reported H_{ads}-Si equilibrium bond length for the monohydride on Si(100)(2×1) surface varies from 1.48 to 1.53 Å.[31-33] We take 1.514 Å.[31] The Si-Si dimer bond distance, d_{SiSi}, is taken as 2.52 Å.[31] The Si-Si distance between the adjacent dimer bonds is d_{SiSi}' = 3.87 Å and the nearest Si-Si distance between two adjacent dimer strands is d_{SiSi}'' = 5.15 Å.[31]

The potential and spectroscopic constants for the $H_{gas}\cdots H_{ads}$ interaction are[34] $D_{HH} = D^0_{0,111} + 1/2\hbar\omega_{HH}$ = 4.751 eV, $D^0_{0,111}$ = 4.478 eV, $a_{HH} = (D_{HH}/2\mu_{HH})^{1/2}/\omega_{HH}$ = 0.257 Å, $\omega_{HH}/2\pi c$ = 4401 cm^{-1}, $r_{HH,e}$ = 0.741 Å and $\mu_{HH} = 1/2m_H$. In addition to the latter interaction, the reaction-zone interaction is dependent upon the instantaneous coordinates of the H_{ads}-Si bond and the displacement of the 0th surface atom. Since the coordinate of the surface atom in surface normal direction is displaced by ξ_0 from its equilibrium position, we include the coordinate of the 0th atom, ξ_0, in the distance between the adatom and the 0th atom as $r_{HSi} = r_{HSi,e} - \xi_0$. Thus, the H_{ads}-Si interaction is directly coupled to the N-atom chain. The H_{ads}-Si potential and spectroscopic constants are $D_{HSi} = D^0_{0,HSi} + 1/2\hbar\omega_{HSi}$ = 3.630 eV, $D^0_{0,HSi}$ = 3.50 eV,[35,36] $a_{HSi} = (D_{HSi}/2\mu_{HSi})^{1/2}/\omega_{HSi}$ = 0.334 Å, $\omega_{HSi}/2\pi c$ = 2093 cm^{-1}.[22,37] Here μ_{HSi} is the reduced mass associated with the H_{ads}-Si bond. The x- and y-direction vibrational energies are known as 645 cm^{-1}.[37] For the H_{gas}-surface interaction, we take D_{HS} = 0.0433 eV,[38] a_{HS} = 0.40 Å.[30] We also take the equilibrium separation as 3.38 Å.[38]

For this reaction, the activation energy is known to be only ~1.0 kcal/mole.[11,12,26] After varying values of the Sato parameter Δ's systematically, we find that the set Δ_{HH} = 0.20, Δ_{HSi} = 0.20 and Δ_{HS} = 0.40 for the reaction zone Si atom (*i.e.*, the H_{gas} to 0th Si atom) and Δ_{HS} = 0.10 for the H_{gas} to remaining eight surface-layer Si atoms, describe best the desired features, minimizing the barrier height and the attractive well in the product channel. The resulting LEPS potential energy surface is shown in Figure 2 for $\theta = \phi = 0$ and b = 0. The barrier height on this surface is 1.3 kcal/mol. Once the PES is constructed, we can follow the time evolution of the primary system atoms by integrating the equations which describe the motions of reaction-zone and N chain atoms. We expect that this PES which includes pertinent primary-zone coordinates will enable us to understand

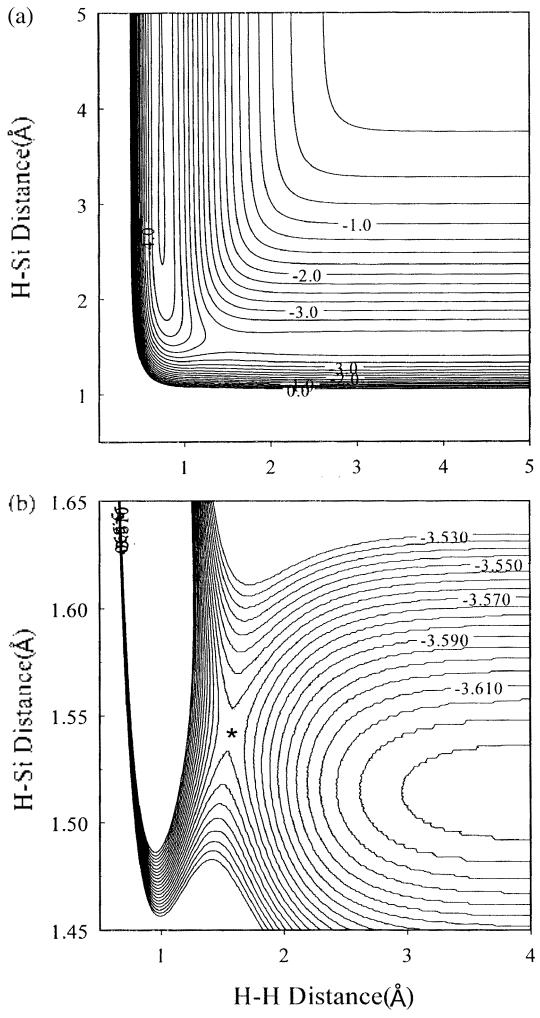

Figure 2. Potential energy surface in (a) coarse scale and (b) fine scale in the region of energy barrier. The contour plots are for the case of $\theta = \phi = 0$, and $b = 0$. The contour labels are in eV.

how gas atoms with given initial conditions react with chemisorbed atoms and then desorb from the surface.

We use a united set of the equations of motion for the reaction-zone atoms and N chain atoms using the Langevin approach to couple the primary system to the heat bath. The gas-adatom part of the resulting equations are

$$\mu\ddot{Z}(t) = -\partial U(r_{HSi}, \phi, \rho, Z, \Phi, \{\xi\})/\partial Z, \quad (4a)$$

$$\mu_{HSi}\ddot{r}(t) = -\partial U(r_{HSi}, \phi, \rho, Z, \Phi, \{\xi\})/\partial r_{HSi}, \quad (4b)$$

$$\mu_{HH}\ddot{\rho}(t) = -\partial U(r_{HSi}, \phi, \rho, Z, \Phi, \{\xi\})/\partial \rho, \quad (4c)$$

$$I_{HSi}\ddot{\theta}(t) = -\partial U(r_{HSi}, \phi, \rho, Z, \Phi, \{\xi\})/\partial \theta, \quad (4d)$$

$$I_{HSi}\ddot{\phi}(t) = -\partial U(r_{HSi}, \phi, \rho, Z, \Phi, \{\xi\})/\partial \phi, \quad (4e)$$

$$I_{HH}\ddot{\Phi}(t) = -\partial U(r_{HSi}, \phi, \rho, Z, \Phi, \{\xi\})/\partial \Phi, \quad (4f)$$

where μ is the reduced mass of the collision and I is the moment of inertia of the diatomic species indicated.

The surface part consists of

$$M_s\ddot{\xi}_0(t) = -M_s\omega_{c0}^2\xi_0(t) - M_s\omega_{c1}^2\xi_1(t) - \partial U(r_{HSi}, \theta, \phi, \rho, Z, \Phi, \{\xi\})/\partial \xi_0 \quad (5a)$$

$$M_s\ddot{\xi}_j(t) = -M_s\omega_{cj}^2\xi_j(t) + M_s\omega_{cj}^2\xi_j(t) - M_s\omega_{c,j-1}^2\xi_{j-1}(t), \quad j = 1, 2, \ldots, N-1 \quad (5b)$$

$$M_s\ddot{\xi}_N(t) = -M_s\Omega_N^2\xi_N(t) - M_s\omega_{c,N}^2\xi_{N-1}(t) - M_s\beta_{N-1}\dot{\xi}_N(t) + M_s f_{N-1}(t), \quad (5c)$$

In Eq. (5c), Ω_N is the adiabatic frequency. That is, at short times the jth oscillator responds like an isolated harmonic oscillator with frequency ω_{cj}, whereas Ω_N determines the long-time response of the heat bath. The friction coefficient β_{N+1}, which enters in the effective equation of motion, Eq. (5c), governs the dissipation of energy from the primary zone to the heat bath, the process which occurs a long time after reaction.[30,39] The values of β_{N+1} are very close to $\pi\omega_D/6$, where ω_D is the Debye frequency. The Debye temperature of the Si crystal is 640K.[40] All values of β and those of ω_c, ω_c, and Ω are presented elsewhere.[39] The quantity $M_s f_{N-1}(t)$ is the stochastic or random force on the primary system arising from thermal fluctuation in the heat bath and balances, on average, the dissipative force, $M_s\beta_{N+1}\dot{\xi}_N(t)$, which removes energy from the primary system in order that the equilibrium distribution of energies in the primary system be restored after collision. The random force term is white noise whose fluctuations are governed by a Markovian fluctuation-dissipation theorem $< f_{N+1}(t) \cdot f_{N+1}(0) > = (6kT_s/M_s)\beta_{N+1}\delta(t)$.[28]

Results and Discussion

The computational procedures include an extensive use of Monte Carlo routines to generate random numbers for initial conditions. The first of them is to sample collision energies E from a Maxwell distribution at the gas temperature T_g. We sample 30,000 values of E. In sampling impact parameters b, we note that the distance between the hydrogen atoms adsorbed on the nearest sites is 3.59 Å. Thus, we take the half-way distance so that the flat sampling range is $0 \leq b \leq 1.80$ Å (*i.e.*, $b_{max} = 1.80$ Å). In the collision with $b > 1.80$ Å, the gas atom is now in the interaction range of the hydrogen atom adsorbed on the adjacent surface site. The initial conditions and numerical techniques needed in solving the equations of motions are given in detail elsewhere.[30]

Throughout this paper, we take $N = 9$; *i.e.*, the adsorbed hydrogen atom is bound to the $(N+1) = 10$ solid atom chain. We have selected this chain length after checking the dependence of energy transfer to the solid as a function of chain length.[39] From the calculation of the reaction probability, we find the N dependence to be insignificant beyond $(N+1) = 10$, where the reaction probability at the gas and the surface temperature (T_g, T_s) is defined as the ratio of the number of reactive trajectories N_R to the total number of trajectories N_T sampled over the entire range of impact parameters; $P(T_g, T_s) = N_R/N_T$. At the thermal conditions of (T_g, T_s) = (1800, 300 K), 2274 trajectories out of a total of 30000 sampled are found to be reactive (*i.e.*, $P = 0.0758$). Note that the gas temperature of 1800 K is known to be the typical experimental condition for producing hydrogen atoms. Most of these reac-

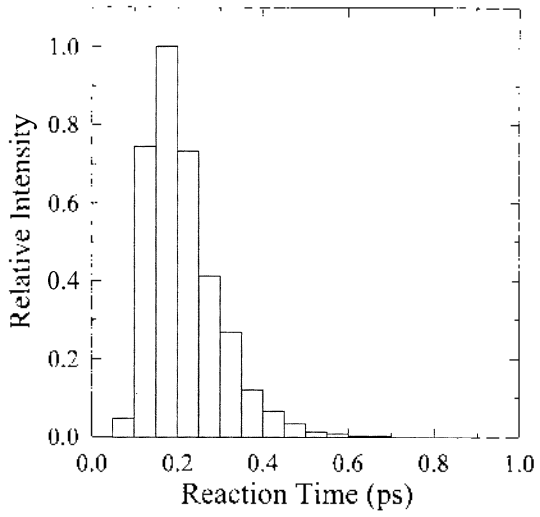

Figure 3. Reaction time distribution

tive events occur on a subpicosecond scale during which the adatom suffers only one impact with the surface, and the ensemble-average of reaction times for the reactive collisions is 0.22 ps (see Figure 3). At this thermal condition, there is no evidence of the gas atom trapping on the surface. Thus we regard all these short-time direct-mode events to follow the ER mechanism, in which the incident atom cannot accommodate to the surface temperature on such a fast time scale.

In order to find out the reason why the reaction occurs so fast, let us examine in detail some of the typical reaction trajectories. We look into several important aspects of the dynamics of this reaction. Figure 4a, shows the H_{ads}-Si, H_{gas}-Surface and H_{ads}-H_{gas} distances for the representative trajectory. Before collision, H_{ads}-Si bond undergoes a highly regular vibration at 2093 cm^{-1}. The H_{gas} to H_{ads} distance also oscillates by the same frequency as the adatom vibration affects the H_{gas} to H_{ads} distance. Near t = 0.1 ps the incident H_{gas} suffers impact with the adatom, forming H_2. The H_2 formation is clearly seen from the highly organized vibrational motion of the H_{gas}-H_{ads} distance around its equilibrium value of approximately 0.75 Å, as well as from the divergence of the H_{ads}-Si distance. The crossing of H_{ads}-Si and H_{gas}-Surface distance curves is due to the rotation of the desorbing H_2 molecule. The H_{gas}-H_{ads} interaction energy begins with 4.75 eV, which then begins to decrease near $t = 0.10$ ps. This moment can be identified as the start of interaction (see Figure 4b). It begins to decrease rapidly near $t = 0$, reaching almost zero, while the H_{ads}-Si vibrational energy rapidly rises to the H_{ads}-Si dissociation threshold of 3.63 eV. Figure 4b clearly shows an efficient exchange flow of energy from the H_{gas} to H_{ads} interaction to the H_{ads}-Si vibration during a brief period of about 0.3 ps. Figure 4b also shows that the vibrational energy of H_2 finally settles to a constant value of 0.726 eV. Since the exchange flow of energy from the H_{gas} to H_{ads} interaction to the H_{ads}-Si vibration occurs in a very brief period, the reaction time becomes very short. Since impact occurs at $t = 0.12$ ps, the reaction time for this representative event can be determined as 0.36 ps. As noted above, the collision begins at $t = -0.10$ ps, so the duration of collision can be determined as 0.46 ps.

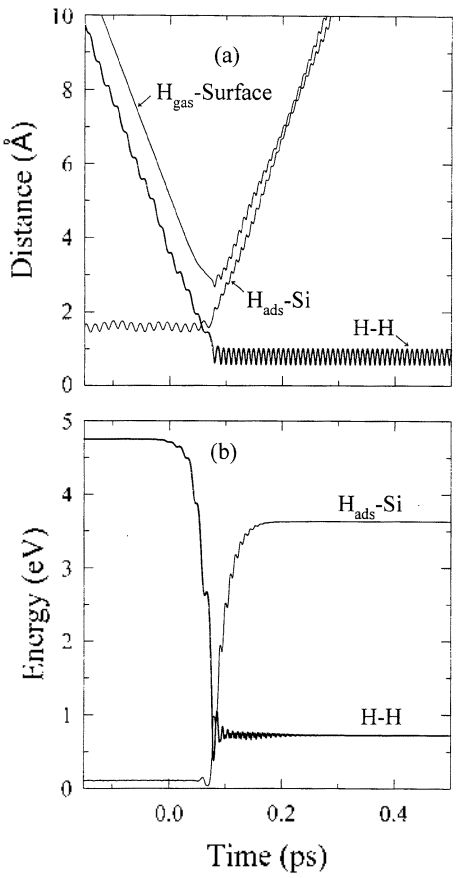

Figure 4. Dynamics of the representative trajectory at (1800, 300 K). (a) The time evolution of the H_{gas}-surface, H_{gas}-H_{ads}, and H_{ads}-Si distances and (b) the H_{gas}-H_{ads} interaction energy and the H_{ads}-Si vibrational energy. In (b) the initial value of the H_{gas}-H_{ads} interaction is D_{HH} and the final value of the H_{ads}-Si vibration energy is the dissociation threshold D_{HSi}.

On the other hand, the decrease of the H_{gas} to H_{ads} interaction and the increase of the H_{ads}-Si bond energy occurs stepwise in concert with each other. In the present mass distribution of **L + LH**, the light incident atom initially trapped in the upper region of the potential well rapidly cascades down the well through ladder-climbing (or declimbing) processes in which the $H_{gas}\cdots H_{ads}$ interaction loses its energy in a series of small steps. This stepwise deactivation was also observed in the **H + LH** case (e.g., Cl + H/Si reaction),[41] in which the light atom oscillates between the two heavy atoms. On the contrary, in the **L + HH** case (e.g., the H + Cl/Si reaction),[30] the process of deactivation occurs in a single-step process. In this **L + LH** case, however, the activation in the H_{ads}-Si bond energy also occurs in a series of small steps. This stepwise activation was not observed in **H+ LH** or **L+ HH** cases.

The probability $P(T_g, T_s)$ defined above is a total probability at the specified thermal conditions of T_g and T_s. However, it is also important to analyze the dependence of the extent of reaction on the impact parameter. In Figure 5a, we show

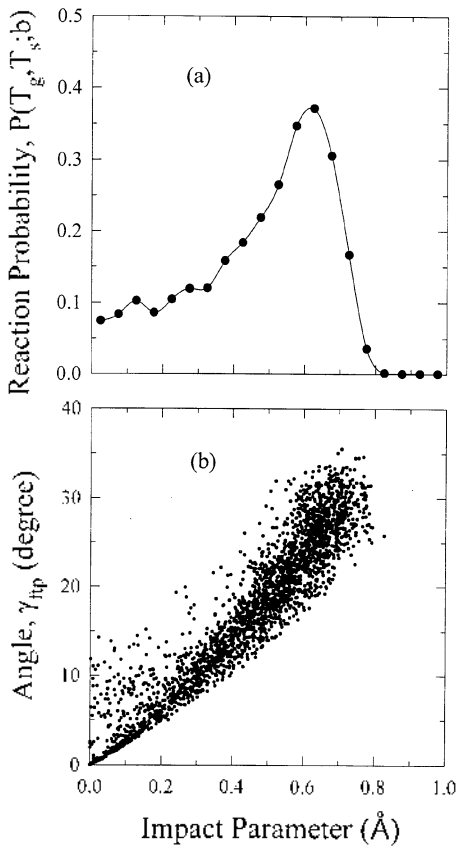

Figure 5. (a) Dependence of the reaction probability $P(T_g, T_s; b)$ upon the impact parameter. (b) Relationship between the incident angle at the first turning point, γ_{flip} and the impact parameter b. Both plots are for the thermal condition (1800, 300 K).

the b-dependent reaction probability $P(T_g, T_s; b)$. To determine this probability, we have counted reactive trajectories in intervals of $b = 0.05$ Å and divided the number of such trajectories $N_R(b)$ by the number of trajectories $N(b)$ sampled in the same interval. As shown in Figure 5a, the probability $P(T_g, T_s; b)$ is small in $b = 0$ collisions and then takes the maximum near $b = 0.6$ Å. It then rapidly decreases as the impact parameter increases and becomes zero at $b = 0.8$ Å. Since the nearest Si-Si distance is 3.59 Å, the region of influence exerted by the adatom on the incident gas atom is a hemisphere with the radius 1/2(3.59 Å). Thus, the occurrence of reactive events in the narrow range of $0 \leq b \leq 0.8$ Å clearly indicates their confinement to the immediate neighborhood of the adatom site. Such localized reactivity has been observed in the hydrogen abstraction reaction on silicon by other gas-phase atoms (Cl or D).[41,42] From the b-dependent reaction probability we can calculate the total reaction cross section of 0.435 Å^2 from the expression defined as $\sigma = 2\pi\int_0^{b_{max}} P(T_g, T_s; b) b\, db$. It may be noted that Caratzoulas *et al.* also obtained a very similar value for σ(0.46 Å^2) from their quasiclassical trajectory study of H + H/Cu(111) system.[43] But, our reaction cross section is far smaller than that of Kratzer (~25 Å^2) for the similar systems, H + D/Si(001) and D + H/Si(001) reaction,[17] because he considered the reactions by a direct Eley-Rideal reaction and mediated by a "hot precursor" and induced desorption of homonuclear molecules, whereas we only consider a direct Eley-Rideal reaction.

In order to explain the fact that the probability $P(T_g, T_s; b)$ shows the maximum near $b = 0.6$ Å, we consider the angle between the $H_{gas}\cdots H_{ads}$ direction and the normal axis through H_{ads} at the instant of impact (*i.e.*, γ_{flip} at the first turning point). As shown in Figure 5b, this angle depends approximately linearly on the impact parameter in a narrow range of $\gamma_{flip} = 0$-35° (b=0-0.8 Å). This figure shows that the angle near $b = 0.6$ is approximately 20°, which is equal to the tilted angle of the adatom. From this we can conclude that the reaction probability is highest when H_{gas} atom approaches the H_{ads} atom collinearly with the H_{ads}-Si bond. In the collinear $H_{gas}\cdots H_{ads}\cdots$Si configuration, the energy flow from H_{gas}-H_{ads} interaction to H_{ads}-Si interaction is most efficient and in turn, the H_{ads}-Si bond gains sufficient energy to dissociate most easily. Our result is in agreement with Takamine and Namiki's experimental finding that the angular distribution of HD product peaks somewhere between 18° and 25° from the surface normal in D + H/Si(100) reaction.[25]

The exothermicity of the gas-phase H + H → H_2 formation is 4.48 eV, whereas D_0^0 for the H_{ads}-Si surface is 3.50 eV. In the ER reaction, the reactant state is H(g)+H(ad), which is thus about 1.0 eV above the H_2(g) state, *i.e.*, the reaction to form H_2(g) is exothermic by this amount. Other energies available for the product state are the collision energy of the incident gas atom E (on the average 0.23 eV at 1800 K), the initial energy of the H_{ads}-Si vibration and the initial energy of the solid. The H_{gas} to H_{ads} interaction energy starts out with D_{HH} and rapidly decreases. For the representative trajectory, it was shown that the vibrational energy of H_2 finally settles to a constant value of 0.726 eV in Figure 4b. The dependence of H_2 vibrational energy on the impact parameter is shown in Figure 6a. As shown in this figure, the general features are that the H_2 molecules produced in small b collisions are vibrationally excited and the extent of vibrational excitation decreases as the impact parameter increases toward 0.8 Å. The mean vibrational energy of the desorbed H_2 molecules is 0.735 eV. On the other hand, as noted above, the number of reactive events is also small in $b = 0$ collisions and then takes the maximum near $b = 0.6$ (see Figure 5a). Due to these two opposing trends, as shown in Figure 6b, the vibrational population distribution is inverted with the maximum appearing near the vibrational energy 1.1 eV. From the eigenvalue expression $E_{vib}(v) = hc\omega_e(v + 1/2) - hc\omega_e x_e(v + 1/2)^2$ with $\omega_e = 4401$ cm^{-1}, $\omega_e x_e = 121.3$ cm^{-1}, we find the vibrational energies 0.273, 0.819, 1.364 and 1.910 eV for $v = 0$, 1, 2 and 3, respectively. The comparison of these energies with the energy scale used in Figure 6b indicates that about 60% of the product molecules have their vibrational energies close to $v = 1$. The similar vibrational population inversion has been found in OH produced from the recombination of gas-phase oxygen atom and chemisorbed hydrogen atom on a tungsten surface,[44,45] and in CO_2 produced from the reaction of oxygen atom with chemisorbed CO on a plat-

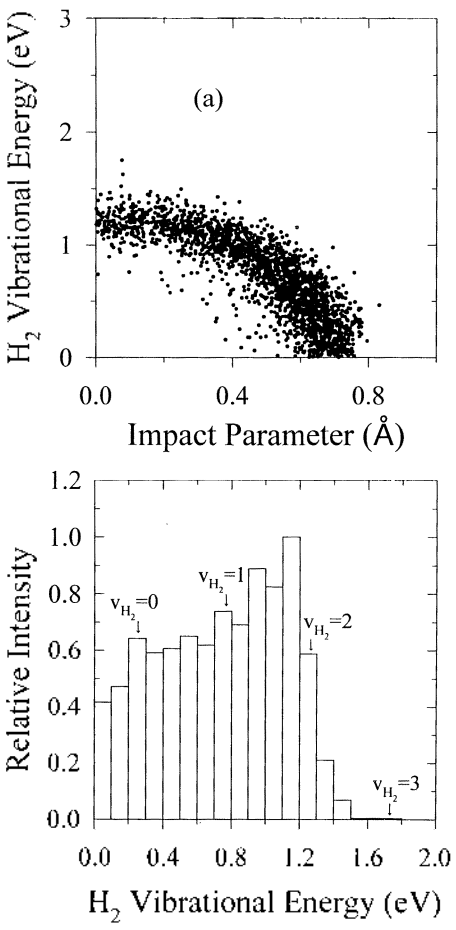

Figure 6. Distribution of the vibrational energy at (1800, 300 K): (a) dependence of the vibrational energy upon the impact parameter; (b) vibrational population distribution. The vibrational energies corresponding to v_{H_2} = 0, 1, 2, and 3 are indicated.

inum surface.[39]

The amount of energy deposited in the translational motion of H_2 is smaller than the vibrational energy. The ensemble averaged translational energy is 0.195 eV. Figure 7 shows the translational energy distribution. Even though the distribution looks to be shifted toward low energy range, it still is of a non-Boltzmann type distribution with ensemble averaged energy far greater than the thermal average $3/2kT_s$ (0.039 eV). This means that the product molecules do not have sufficient time to equilibrate with the surface temperature.

The amount of energy taken up by the rotational motion of the H_2 molecule is very small, in contrast to the translational and vibrational motions. The ensemble-averaged rotational energy is only 0.118 eV. This implies that H_2 rotation does not play an important role in the desorption process. In the case of Cl(g) + H(ad)/Si → HCl(g) + Si reaction,[41] however, the reaction energy carried by the rotatinal motion of the product molecule is quite significant. In the latter reaction, the heavy incident atom can approach the solid surface closer than the light incident atom. This produces more torque in the desorbing HCl molecule and, thus, increases the rotational energy.

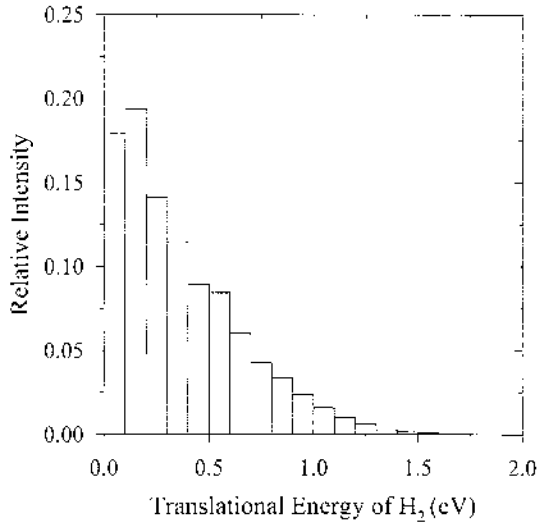

Figure 7. Translational population distribution at (1800, 300 K). Note that $3/2kT_s$ = 0.039 eV.

The amount of energy transfer to the silicon surface is small because of the large difference between the masses of H and Si. At the thermal conditions (1800, 300 K), the ensemble-average of energy transfer to the surface is 0.131 eV. It is interesting to note that the amount of energy propagated into the solid involving heavy chemisorbed atoms such as chlorine is significantly larger than that of the present process.[30]

Figure 8a shows a moderate dependence of the reaction probability on the surface temperature. At the gas temperature of 1800 K, the probability decreases slowly from 0.084 at T_s = 0 K to 0.076 at T_s = 700 K, but the effect of the surface temperature on the reaction is negligible. This is a typical result for an ER process. Jackson *et al.* explained the surface temperature dependence in terms of an increased reactivity as the adsorbate becomes vibrationally excited.[46] In this work, however, the H_{ads}-Si vibrational frequency is quite high (2093 cm^{-1}), and the fraction of vibrationally excited states is only 0.013 even at T_s = 700 K, thus playing no significant role in the reaction. The magnitude of the reaction probability, as well as its temperature dependence, are comparable to those of Koleske *et al.*[12] They reported the overall probability as 0.109 which is somewhat larger than our result, 0.076. In their theoretical model, however, they only considered collinear geometry collisions ignoring the effect of impact parameter and rotational motion, and fixed the incident H atom kinetic energy at 0.03 eV. These probabilities are also comparable with those of the another related reaction H(g) + Cl(ad)/Si. But, these probabilities are significantly lower than those of the related reaction Cl(g) + H(ad)/Si. For example, at the thermal conditions of (1800, 300 K), the probability of H_2 formation in H(g) + H(ad)/Si is 0.076, whereas that of HCl formation in Cl(g) + H(ad)/Si is 0.179 at (1800, 300 K). This indicates that the abstraction of light hydrogen atom by light hydrogen atom is more difficult than by heavier chlorine atom. As shown in Figure 8b, the dependence of the reaction probability on T_g is much stron-

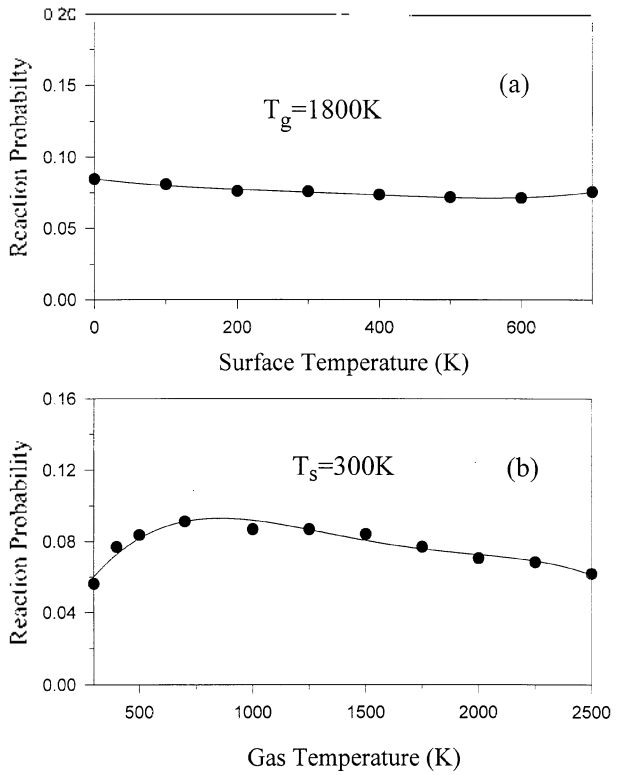

Figure 8. Dependence of the reaction probability $P(T_g, T_s)$ on the gas and surface temperatures. (a) Dependence on the surface temperature for the gas temperature fixed at 1800 K and (b) dependence on the gas temperature for the surface temperature fixed at 300 K.

ger than the surface temperature dependence. The results for a fixed surface temperature of 300 K show the reaction probability rising rapidly with the gas temperature in the range of T_g ~ 300 to 700 K, beyond which it decreases slightly with increasing temperature. The variation of reaction probability at lower temperatures follows a general thermal effect that the extent of a chemical reaction increases with increasing temperature. The rise is a result of the incident atoms having greater collision energies according to the Maxwellian distribution. But, at higher temperatures, where high energy collisions dominate, the fast moving gas atom does not stay on the surface long enough to allow reaction. Furthermore, since the barrier height is very small (≈ 0.05 eV), further increase in T_g (or E) does not affect the extent of reaction significantly as the collision energy in most of the ER reactive events has already surpassed the barrier height. Thus, a larger number of trajectories leave the surface without reaction, so the reaction probability decreases at high temperatures, exhibiting an negative temperature dependence.

Concluding Comments

The reaction probability for the gas-surface reaction H(g) + H(ad)/Si → H_2(g) + Si through the Eley-Rideal mechanism is shown to be not large. The reaction probability is independent of the surface temperature between 0 and 700 K, whereas its dependence on the gas temperature is significant. The largest value the reaction probability can take is about 0.1 near the gas temperature of 700 K.

Most reactive events occur on the subpicosecond time scale, following the direct-mode collision between the incident gas atom and the adatom. The distribution of reactive events is localized in the immediate neighborhood of the adatom site on the surface.

Most of the reaction exothermicity deposits in the product vibration, followed by translation. The amount of the reaction energy dissipated into the surface is small. Furthermore, the amount of energy shared by the rotational motion is much smaller, implying that H_2 rotation does not play an important role in the desorption process.

Acknowledgment. The authors wish to acknowledge the financial support of the Korea Research Foundation made in the program year of 1997.

References

1. Bortolani, V.; March, N. H.; Tosi, M. P. Eds., *Interaction of Atoms and Molecules with Solid Surfaces*; Plenum Press: New York, 1990.
2. Rettner, C. T.; Ashfold, M. N. R. Eds., *Dynamics of Gas-Surface Interactions;* Royal Soc. of Chemistry, Thomas Graham House: Cambridge, 1991.
3. Somorjai, G. A. *Introduction to Surface Chemistry and Catalysis*; Wiley: New York, 1994.
4. Brivio, G. P.; Grimley, T. B. *Surf. Sci. Rep.* **1993**, *17*, 1.
5. Cheng, C. C.; Lucas, S. R.; Gutleben, H.; Choyke, W. J.; Yates, J. T., Jr. *J. Am. Chem. Soc.* **1992**, *114*, 1249.
6. Cheng, C. C.; Lucas, S. R.; Gutleben, H.; Choyke, W. J.; Yates, J. T., Jr. *Surf. Sci. Lett.* **1992**, *273*, L441.
7. Weakliem, P. C.; Wu, C. J.; Carter, E. A. *Phys. Rev. Lett.* **1992**, *69*, 200.
8. Yates, J. T., Jr.; Cheng, C. C.; Gao, Q.; Choyke, W. J. *Surf. Sci. Rep.* **1993**, *19*, 79.
9. Koleske, D. D.; Gates, S. M. *J. Chem. Phys.* **1993**, *98*, 5091; **1993**, *99*, 8218.
10. Koleske, D. D.; Gates, S. M. *J. Appl. Phys.* **1993**, *74*, 4245.
11. Koleske, D. D.; Gates, S. M.; Schultz, J. A. *J. Chem. Phys.* **1993**, 99, 5619.
12. Koleske, D. D.; Gates, S. M.; Jackson, B. *J. Chem. Phys.* **1994**, *101*, 3301.
13. Durbin, T. D.; Simpson, W. C.; Chakarian, V.; Shuh, D. K.; Varekamp, P. R.; Lo, C. W.; Yarmoff, J. A. *Surf. Sci.* **1994**, *316*, 257.
14. Liu Q.; Hoffman, R. *J. Am. Chem. Soc.* **1995**, *117*, 4082.
15. Waltenburg, H. N.; Yates, J. T., Jr. *Chem. Rev.* **1995**, *95*, 1589.
16. Doren, D. J. *Adv. Chem. Phys.* **1996**, *95*, 1.
17. Kratzer, P. *J. Chem. Phys.* **1997**, *106*, 6752.
18. NoorBatcha, I.; Raff, L. M.; Thompson, D. L. *J. Chem. Phys.* **1985**, *83*, 1382.
19. Sinniah, K.; Sherman, M. G.; Lewis, L. B.; Weinberg, W. H. *J. Chem. Phys.* **1990**, *92*, 5700.
20. Kolasinski, K. W.; Shane, S. F.; Zare, R. N. *J. Chem. Phys.* **1991**, *95*, 5482.
21. Nachtigall, P.; Jordan, K. D.; Sosa, C. *J. Phys. Chem.* **1993**, *97*, 11666.

22. Flowers, M. C.; Jonathan, N. B. H.; Liu, Y.; Morris, A. *J. Chem. Phys.* **1993**, *99*, 7038.
23. Widdra, W.; Yi, S. I.; Maboudian, R.; Briggs, G. A. D.; Weinberg, W. H. *Phys. Rev. Lett.* **1995**, *74*, 2074.
24. Srinivasan, E.; Yang, H.; Parsons, G. N. *J. Chem. Phys.* **1996**, *105*, 5467.
25. Takamine, Y.; Namiki, A. *J. Chem. Phys.* **1997**, *106*, 8935.
26. Buntin, S. A. *J. Chem. Phys.* **1996**, *105*, 2066; **1998**, *108*, 1601.
27. Tully, J. C. *J. Chem. Phys.* **1980**, *73*, 1975.
28. Adelman, S. A. *J. Chem. Phys.* **1979**, *71*, 4471.
29. Adelman, S. A. *Adv. Chem. Phys.* **1980**, *44*, 143.
30. Kim, Y. H.; Ree, J.; Shin, H. K. *J. Chem. Phys.* **1998**, *108*, 23.
31. Radeke, M. R.; Carter, E. A. *Phys. Rev. B* **1996**, *54*, 11803.
32. Chabal, Y. J.; Raghavachari, K. *Phys. Rev. Lett.* **1984**, *53*, 282; **1985**, *54*, 1055.
33. Zheng, X. M.; Smith, P. V. *Surf. Sci.* **1992**, *279*, 127.
34. Huber, K. P.; Herzberg, G. *Constants of Diatomic Molecules*; Van Nostrand Reinhold: New York, 1979.
35. Van de Walle, C. G.; Street, R. A. *Phys. Rev. B* **1995**, *51*, 10615.
36. Kratzer, P.; Hammer, B.; Norskov, J. K. *Phys. Rev. B* **1995**, *51*, 13432.
37. Tully, J. C.; Chabal, Y. J.; Raghavachari, K.; Bowman, J. M.; Lucchese, R. P. *Phys. Rev. B* **1985**, *31*, 1184.
38. Ghio, E.; Mattera, L.; Salvo, C.; Tommasini, F.; Valbusa, U. *J. Chem. Phys.* **1980**, *73*, 556.
39. Ree, J.; Kim, Y. H.; Shin, H. K. *J. Chem. Phys.* **1996**, *104*, 742.
40. Gray, D. E., Ed.; *American Institute of Physics Handbook*, 3rd ed.; McGraw-Hill: New York, 1972; p 4-116.
41. Kim, W. K.; Ree, J.; Shin, H. K. *J. Phys. Chem. A* **1999**, *411*, 103.
42. Eenshuistra, P. J.; Bonnie, J. H. M.; Los, J.; Hopman, H. J. *Phys. Rev. Lett.* **1988**, *60*, 341.
43. Caratzoulas, S.; Jackson, B.; Persson, M. *J. Chem. Phys.* **1997**, *107*, 6420.
44. Ree, J.; Shin, H. K. *Chem. Phys. Lett.* **1996**, *258*, 239.
45. Ree, J.; Kim, Y. H.; Shin, H. K. *J. Phys. Chem. A* **1997**, *101*, 4523.
46. Jackson, B.; Persson, M.; Kay, B. D. *J. Chem. Phys.* **1994**, *100*, 7687.